INTERNATIONAL JOURNAL OF INNOVATIVE RESEARCH & DEVELOPMENT

ISSN 2278 – 0211 (Online)

Intense Two Photon Green-Red Upconversion in Er^{3+}/Yb^{3+}/KF/BaO Doped Perovskite $SrTiO_3$ Glass Ceramic

Aditya Maheshwari
Department of Ceramic Engineering, Indian Institute of Technology
Banaras Hindu University, Varanasi, India
S. B. Rai
Department of Physics, Faculty of Science, Banaras Hindu University, Varanasi, India
Om Parkash
Department of Ceramic Engineering, Indian Institute of Technology
Banaras Hindu University, Varanasi, India
Devendra Kumar
Department of Ceramic Engineering, Indian Institute of Technology
Banaras Hindu University, Varanasi, India

Abstract:
Er^{3+}/Yb^{3+} doped perovskite $SrTiO_3$ matrix was crystallized in borosilicate glass ceramic in order to investigate its optical properties. Powder x-ray diffraction analysis showed two major crystalline phases $SrTiO_3$ and β-TiO_2, present in the glass ceramic. Particle size in crystalline matrix, calculated by Scherrer's formula lies in the range of 50-100nm, which was confirmed by SEM micrographs later. Emission spectra of both glass and glass ceramic consisted of two intense green and one red band. Upconversion in glass ceramic was found around 10 times more intense than that in glass. Power dependence studies suggested that 2 excitation photons are participating in various upconversion mechanisms. Transitions $^2H_{11/2}/^4S_{3/2} \rightarrow {}^4I_{15/2}$ and $^4F_{9/2} \rightarrow {}^4I_{15/2}$, responsible for green and red emissions respectively, were visualized through excited state absorption and energy transfer mechanisms.

Key words: *upconversion, glass ceramic, luminescence, energy transfer*

1. Introduction

There has been a renaissance in the study of various perovskite materials for their dielectric (Anderson, 1992; Thakur, Prakash, & James, 2009), optical (Guo et al., 2006; Patra, Friend, Kapoor, & Prasad, 2003) and other structural properties (Battisha, Speghini, Polizzi, Agnoli, & Bettinelli, 2002). These compounds having XYO_3 type structure such as $BaTiO_3$, $SrTiO_3$, and $PbTiO_3$ have drawn a good deal of attention due to their stable structural properties. $BaTiO_3$ and $PbTiO_3$ are ferroelectric perovskites (Cohen & Krakauer, 1992) which possess tetragonal phases at its room temperature, while $SrTiO_3$ is quantum paraelectric and also has high dielectric constant, high charge storage capacity, chemical and physical stability and excellent transparency in the visible range. In addition, its vibrational frequency is quite low making it suitable for host matrix for phosphor materials (Guo, Qiao, Zheng, & Zhao, 2008).

Phosphors with different host matrices have been studied in recent years for their applications in advanced fields. Especially studies on upconversion (UC) phenomenon, an anti-stokes process where long wavelength radiations (IR/NIR region) are converted to shorter wavelengths radiations (UV/visible region) via various multi-photon mechanisms, have made great progress due to their potential applications in upconversion fibers, optical communications, optical temperature sensors, IR sensors, solid state lasers and solar cells (Fischer et al., 2010; Maheshwari, Rai, Parkash, & Kumar, 2011; Xu, Dai, Toth, Del Cul, & Peterson, 1995). UC active nano-crystals are reported for their unique optical and chemical properties, including high quantum yields, very narrow emission peak, large Stokes shifts, high chemical stability, and low toxicity (Heer, Kömpe, Güdel, & Haase, 2004; Liu, Ma, Chen, Yu, & Wang, 2006; Tanabe, Hayashi, Hanada, & Onodera, 2002). A recent study shows that these nano-crystals may also be used as fluorescent labels for sensitive biological detection (Yi et al., 2004; Zhang et al., 2012).UC phenomenon has been observed in various matrices but not very much emphasis has been given to its study in perovskite glass ceramic matrices. Perovskite glass ceramics are known for their special properties as zero or negligible porosity, high strength, opacity, low thermal expansion etc, which encouraged us to investigate an

upconversion active $SrTiO_3$matrix in borosilicate glass ceramic with the doping of Er^{3+} and Yb^{3+} as active and sensitizer ions respectively. Addition of BaO ($BaCO_3$ as raw material) raises the refractive index without increasing the dispersion in glass and KF supports as a modifier and helps to prepare a good crystalline $SrTiO_3$ matrix (Sahu, Kumar, Parkash, Thakur, & Prakash, 2004). During the heat treatment of amorphous SrO-TiO_2 borosilicate glass, small crystallites of $SrTiO_3$ and TiO_2 nucleate and this Internal or external nucleation promotes the development of micro-heterogeneities and crystallization of doped matrix can subsequently begin. As a result, the amorphous parent glass transforms into a uniformly crystalline glass ceramic.

Er^{3+} has the energy levels$^2H_{11/2}$, $^4S_{3/2}$ and $^4F_{9/2}$ responsible for intense green and red UC emission but it is relatively less efficient when singly doped because of its low absorption cross-section in NIR region. To overcome this drawback, co-doping of Yb^{3+}as a sensitizer ion has proven to be a successful alternative to enhance the upconversion processes because of its larger absorption cross-section in NIR. In fact, there is an efficient spectral overlap between the levels$^2F_{5/2}$ (Yb^{3+}) and $^4I_{11/2}$ (Er^{3+}), which provides more energy to Erbium ions via non-radiative energy transfer which in turn enhances the activity of Er^{3+} ion as upconversion centre in the matrix. Energy transfer (ET), excited state absorption (ESA) and photon avalanche are the most common upconversion mechanisms. ESA provides the energy to the excited ion in any meta-stable state and results further excitation of the ion. It requires high pump intensities and not high doping concentrations whereas, high doping densities are usually required in ET process. Photon avalanche was ruled out as a possible mechanism for up conversion because no inflection point was observed in the power study (Vetrone, Boyer, Capobianco, Speghini, & Bettinelli, 2002).

2. Experimental Procedure

In order to synthesize $SrTiO_3$matrix in borosilicate ($2SiO_2.B_2O_3$) glass ceramic, $SrCO_3$, TiO_2, SiO_2, $H_2BO_3$with purity more than 99% were used as starting materials. 0.5 mol% $BaCO_3$ and 0.5 mol% KF were added to have a homogeneous matrix in glass and glass ceramic samples. Rare earth materials Er_2O_3 (0.3wt %) and Yb_2O_3 (2wt %) with purity >99.9% were then added additionally to the mixture. Around 25 g glass batch was melted in alumina crucible and casted in an aluminum die and then annealed at 430°C for 2 hours in annealing furnace. All the heat treatments were performed under air atmosphere. Glass sample was transparent with red-brown color. DTA was recorded with S60/51920-SETARAM Sci. & Industrial Equipment DTA & TGA setup to obtain the glass transition temperature (400°C) and crystallization temperature (830°C). Glass was heat treated at the mentioned crystallization temperature for 3 hours to obtain a homogeneous bulk crystalline glass ceramic. Prepared glass ceramic was opaque with white color. Powder X-ray diffraction (XRD) patterns were recorded using Phillips-PW 1730 Cu Kα radiation to determine the present phases in the samples. Samples were cut into small cuboids having the dimensions around 10×5×2 $mm^3$and polished, etched by using a solution of 2%HF+5% HCl for 20–30 seconds (Thakur, Kumar, Parkash, & Pandey, 2002). Sample surface was coated with Au-Pd using 6.2 HUMMER Sputtering-Anatech Ltd. and micrographs were taken with SUPRA 40, Zeiss Field Emission Scanning Electron Microscope (SEM). Luminescence studies were carried out with the help of iHR320 HORIBA JOBIN YVON Spectrometer and 976nm InGaAs diode laser. Power dependence measurements were carried out with the same set-up.

3. Results and Discussion

3.1. Structural Properties

Powder XRD patterns, shown in Figure.1; indicate that two major phases are present in glass ceramic, $SrTiO_3$ and βTiO_2. It is expected that small amount of rare earth ions replace Sr^{2+} ions from $SrTiO_3$ matrix because of having almost same ionic radii. Theoretically, particle size calculation with the help of Scherrer's formula (Eq. 1) suggests that the particle size of both the phases present in glass ceramic lies in nano range (<100nm). This nano crystallized phase may be one of the major reasons to show the drastic increase in UC emission in glass ceramic. The same effect was also seen in some of the previous works (Maheshwari et al., 2011; Maheshwari, Rai, Parkash, & Kumar, 2013).

$$D_p = 0.94\lambda / \beta_{1/2}\cos\theta \quad (1)$$

Where, λ is wavelength of x-rays used, $\beta_{1/2}$ is full width at half maxima (FWHM) of peaks in the XRD spectrum and 2θ is angle of peak position.

In SEM micrographs of, shown in Figure.2, it may be clearly seen that glass ceramic is made of the bigger particulates (agglomerates), which consists of very small particles. Glass to glass phase separation in the initial stage of heat treatment in similar glass ceramic system might be the possible reason of this microstructure development in glass ceramics (Sahu et al., 2004). Figure. 2(a) shows that the homogeneous distribution of these agglomerates over the surface as well as in bulk whereas, in Figure. 2(b), very dense packing of the small particles (in nano range) within the agglomerates may be observed at higher magnification.

Fourier Transform Infra-Red (FTIR) spectra for both glass and glass ceramic samples are shown in Figure.3. It shows various absorption bands at 709 cm^{-1}corresponding to B-O-B bending vibrations, at 954 cm^{-1}, 1226$cm^{-1}$and 1338 cm^{-1} because of B-O bond stretching of BO_4 units in tri-, tetra-, and penta-borate groups and at 2341cm^{-1}, 2360cm^{-1} corresponding to Si-H (Silane) stretching in glass sample. On the other hand glass ceramic shows small number of absorption bands at 1234 cm^{-1} and 1375 cm^{-1} because of B-O stretching of trigonal BO_3 units in boroxol rings and at 2360.86 cm^{-1} corresponding to Si-H (Silane) stretching. It is noticeable here that the glass ceramic has lower number of vibrational or stretching bonds than in glass which suggests it to have a simple and stable crystalline structure.

3.2. Emission Properties

The intensity distribution among the emission bands depend both on the ion concentration and on host matrix properties. Erbium oxide is a well-known material in the field of UC to work as an optically active dopant in various matrices (Priolo et al., 2001; Steckl & Birkhahn, 1998; van den Hoven et al., 1996). Co-doping of Ytterbium with Erbium oxide plays an important role as a sensitizer ion and produces an efficient upconversion in the samples (Mohanty, Rai, Dwivedi, & Rai, 2011). Emission spectra for both glass and glass ceramic samples with excitation wavelength of 976nm are shown in Figure.4. It consists of the emission lines corresponding to green as well as red emission. Emission lines in green region (520-565nm) are assigned to $^2H_{11/2} \rightarrow {}^4I_{15/2}$ and $^4S_{3/2} \rightarrow {}^4I_{15/2}$whereas, in the red region (625-740 nm) is assigned to $^4F_{9/2} \rightarrow {}^4I_{15/2}$ transitions of Er^{3+} ion. A much more intense UC emission was seen in glass ceramic than that of glass. Similar phenomenon has been seen previously that UC emission increases as the crystallization increases and was highest for the completely crystallized glass ceramics (Maheshwari et al., 2011), which suggests that the dopant ions are optically more active in crystalline phase than in amorphous glass phase. In present case, Er^{3+}/Yb^{3+} ions replace Sr^{2+} ions from the stable $SrTiO_3$crystalline matrix in glass ceramic and participate actively in UC process. In order to have an estimate about the number of photons participating in UC mechanisms i.e. excitation photons, luminescence intensity 'I' of these transitions was measured and plotted in Figure.5. Intensity has the following dependence on laser pump power 'P'.

$$I \alpha P^n \quad (2)$$

Where, n is the number of pumping photons absorbed per emitted photon. Plot of log I vs. log P yields a straight line with slope 'n', which indicates how many photons are contributing to UC emissions in both the glass and glass ceramic samples. Corresponding slopes for green and red emissions suggest the ESA and ET mechanisms to be 2 photons processes via ESA or ET mechanisms i.e. absorption of two exciting wavelength photons takes place to emit one photon of each emitted wavelengths.

3.3. Expected Transitions

Possible UC transitions can be readily determined with the help of power dependence plots. As explained earlier that absorption of 2 electrons (n=2) causes the emission of one photon both for the green and the red emissions. Figure.6 shows the energy level diagram of the active Er^{3+}ion and sensitizer Yb^{3+}ion with possible upconversion transitions. Er^{3+}absorbs one photon of 976nm wavelength and excites from the ground state to $^4I_{11/2}$ level via ground state absorption ($^4I_{15/2} \rightarrow {}^4I_{11/2}$). It excites further to $^4F_{7/2}$state by absorbing another photon via ESA process or by getting the energy transferred from Yb^{3+} via ET process, shown below:

$$^4I_{11/2}(Er^{3+}) + {}^2F_{5/2}(Yb^{3+}) \rightarrow {}^4F_{7/2}(Er^{3+}) + {}^2F_{7/2}(Yb^{3+}) \quad (3)$$

Er^{3+} then undergoes multi-phonon non-radiative relaxation to luminescent levels $^2H_{11/2}$, $^4S_{3/2}$ (both corresponding to green) and $^4F_{9/2}$ (corresponding to red).The decay from these levels to ground level provides the visible emission. The gap bridging between $^4F_{7/2}$ and $^4F_{9/2}$ levels requires more photons and therefore, the above mechanism prefers green emission but red emission is less probable. In order to explain the red emission, another ET process plays an important role which populated $^4F_{9/2}$level (red) directly. In this process, Er^{3+} ions excited via ground state absorption transit to a long living $^4I_{13/2}$ level via non radiative emission. Thereafter, it excites further to populate $^4F_{9/2}$levelby having energy via ESA or ET, shown below:

$$^4I_{13/2}(Er^{3+}) + {}^2F_{5/2}(Yb^{3+}) \rightarrow {}^4F_{9/2}(Er^{3+}) + {}^2F_{7/2}(Yb^{3+}) \quad (4)$$

Radiative decays from $^2H_{11/2}$/ $^4S_{3/2}$and $^4F_{9/2}$to the ground level $^4I_{15/2}$ in Er^{3+}therefore, show green and red emissions respectively. Emission intensity of green emission is seen more than that of red for both the samples and the reason may be the mismatching of $^4I_{13/2}(Er^{3+})$ and $^2F_{5/2}(Yb^{3+})$ levels which leads to a lower amount of energy transfer from Yb^{3+} to Er^{3+} ions.ET process is expected to have larger contribution in UC than ESA process because of the small absorption cross-section of Er^{3+} ions.

4. Conclusion

Two crystalline phases (crystallite size <100nm) $SrTiO_3$ and β-TiO_2 were seen in powder XRD of prepared glass ceramic. The agglomerates of smaller particles were distributed homogeneously in all over the sample. Two intense bands in green region and one broadened band (possibly some merged emission peaks) in red region were seen in UC emission spectra and are assigned to $^2H_{11/2} \rightarrow {}^4I_{15/2}$, $^4S_{3/2} \rightarrow {}^4I_{15/2}$(green) and $^4F_{9/2} \rightarrow {}^4I_{15/2}$(red) transitions. The emission intensity in glass ceramic was found to be around 10 times that in the glass.Two photons process (ESA and ET) were found to be responsible for UC emission.

5. Acknowledgement

Authors acknowledge the help from Prof. S. K. Pratihar from National Institute of Technology, Raurkela for XRD and Mr. Peria Samy from School of Material Science and Technology, IIT-BHU, Varanasi for SEM characterization.

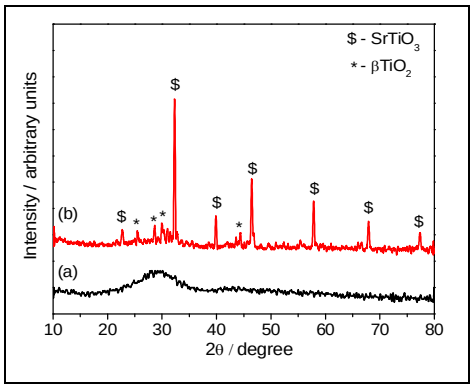

Figure 1: powder X-ray diffraction pattern of (a) glass and (b) glass ceramic with marked peaks

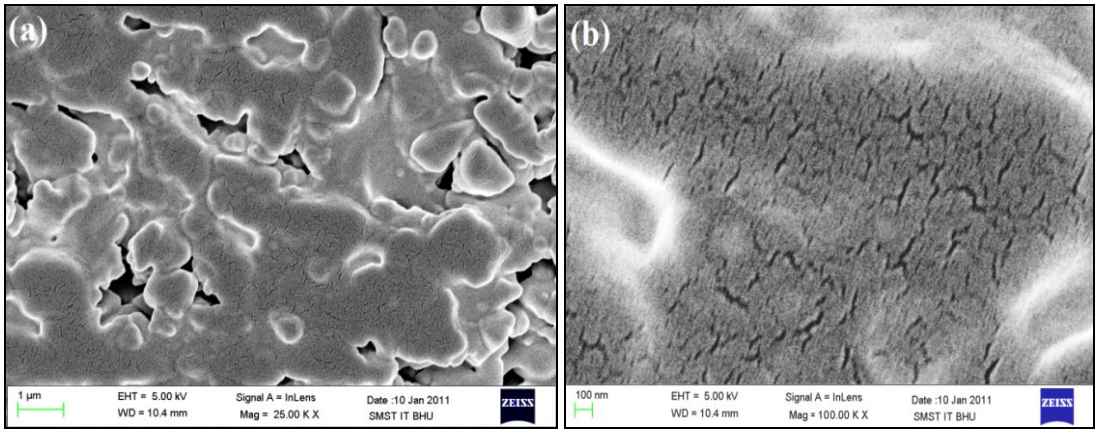

Figure 2: SEM micrographs of glass ceramic sample at (a) 25K× and (b) 100K× magnification

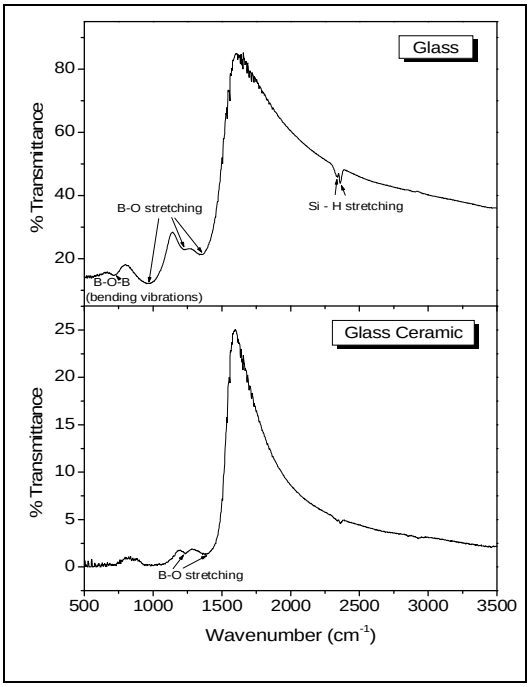

Figure 3: FTIR transmittance spectra for glass and glass ceramic samples

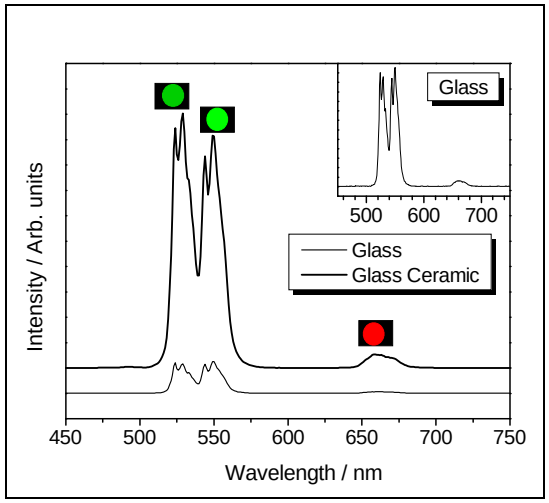

Figure 4: Upconversion emission spectra of glass and glass ceramic samples; Inset: 10× magnified. UC emission spectra for glass; colors shown are only symbolic

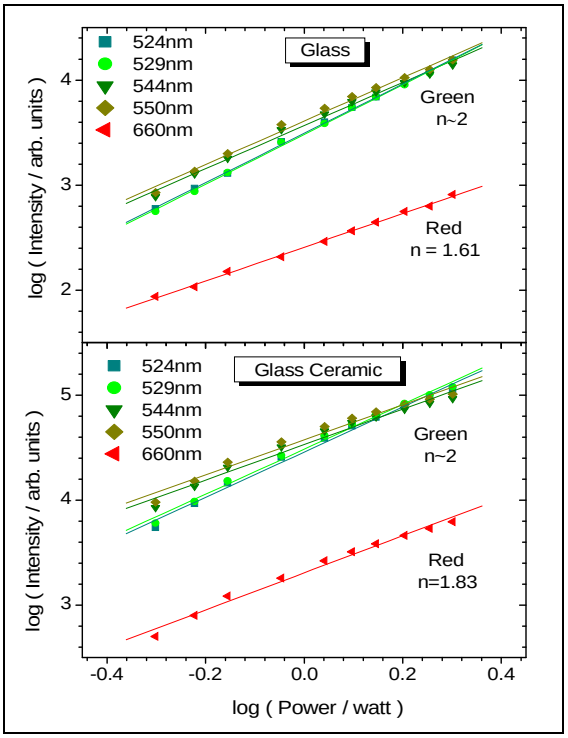

Figure 5: Laser power dependence and corresponding slopes for glass and glass ceramic samples

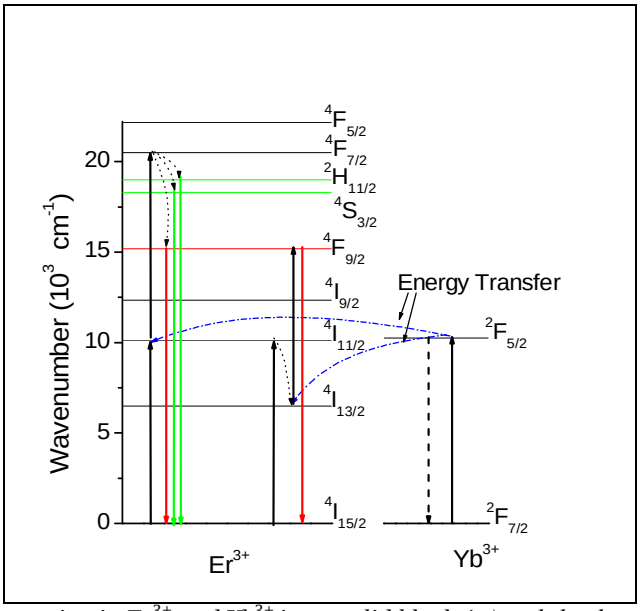

Figure 6: Transition mechanisms occurring in Er^{3+} and Yb^{3+} ions; solid black (—), solid colored(— or —), blue dashed (−·−·−)and dotted (····)lines represent the excitation processes via ESA or ET mechanisms, corresponding colored emission, energy transfer and non-radiative processes respectively

6. References

1. Anderson, H. U. (1992). Review of p-type doped perovskite materials for SOFC and other applications. Solid State Ionics, 52, 33-41.
2. Battisha, I. K., Speghini, A., Polizzi, S., Agnoli, F., & Bettinelli, M. (2002). Molten chloride synthesis, structural characterisation and luminescence spectroscopy of ultrafine Eu3+-doped BaTiO3 and SrTiO3. Materials Letters, 57(1), 183-187. doi: http://dx.doi.org/10.1016/S0167-577X(02)00727-9
3. Cohen, R. E., & Krakauer, H. (1992). Electronic structure studies of the differences in ferroelectric behavior of batio3 and PbTiO3. Ferroelectrics, 136(1), 65-83. doi: 10.1080/00150199208016067
4. Fischer, S., Goldschmidt, J. C., Loper, P., Bauer, G. H., Bruggemann, R., Kramer, K., . . . Glunz, S. W. (2010). Enhancement of silicon solar cell efficiency by upconversion: Optical and electrical characterization. Journal of Applied Physics, 108(4), 044912-044911.
5. Guo, H., Dong, N., Yin, M., Zhang, W., Lou, L., & Xia, S. (2006). Green and red upconversion luminescence in Er3+-doped and Er3+/Yb3+-codoped SrTiO3 ultrafine powders. [doi: 10.1016/j.jallcom.2005.08.008]. Journal of Alloys and Compounds, 415(1–2), 280-283.
6. Guo, H., Qiao, Y.-m., Zheng, J.-f., & Zhao, L.-h. (2008). Upconversion Luminescence of SrTiO 3 :Er 3+ Ultrafine Powders Produced by 785 nm Laser. Chinese Journal of Chemical Physics, 21(3), 233.
7. Heer, S., Kömpe, K., Güdel, H. U., & Haase, M. (2004). Highly Efficient Multicolour Upconversion Emission in Transparent Colloids of Lanthanide-Doped NaYF4 Nanocrystals. Advanced Materials, 16(23-24), 2102-2105. doi: 10.1002/adma.200400772
8. Liu, F., Ma, E., Chen, D., Yu, Y., & Wang, Y. (2006). Tunable Red-Green Upconversion Luminescence in Novel Transparent Glass Ceramics Containing Er: NaYF4 Nanocrystals. [doi: 10.1021/jp063145m]. The Journal of Physical Chemistry B, 110(42), 20843-20846. doi: 10.1021/jp063145m
9. Maheshwari, A., Rai, S. B., Parkash, O., & Kumar, D. (2011). Multi-photon luminescence in Er3+/Yb3+:SrO-TiO2 glass ceramic. Optical Materials, 34(1), 298-302. doi: 10.1016/j.optmat.2011.09.001
10. Maheshwari, A., Rai, S. B., Parkash, O., & Kumar, D. (2013). Effect of crystallization temperature on luminescence behaviour of Er–Yb: SrO·TiO2 borosilicate glass. Journal of Luminescence, 137(0), 1-5. doi: http://dx.doi.org/10.1016/j.jlumin.2012.12.027
11. Mohanty, D., Rai, V., Dwivedi, Y., & Rai, S. (2011). Enhancement of upconversion intensity in Er3+ doped tellurite glass in presence of Yb3+. Applied Physics B: Lasers and Optics, 104(1), 233-236. doi: 10.1007/s00340-011-4422-6
12. Patra, A., Friend, C. S., Kapoor, R., & Prasad, P. N. (2003). Fluorescence Upconversion Properties of Er3+-Doped TiO2 and BaTiO3 Nanocrystallites. Chemistry of Materials, 15(19), 3650-3655. doi: 10.1021/cm020897u
13. Priolo, F., Franzo, G., Pacifici, D., Vinciguerra, V., Iacona, F., & Irrera, A. (2001). Role of the energy transfer in the optical properties of undoped and Er-doped interacting Si nanocrystals. Journal of Applied Physics, 89(1), 264-272. doi: 10.1063/1.1331074
14. Sahu, A. K., Kumar, D., Parkash, O., Thakur, O. P., & Prakash, C. (2004). Effect of K2O/BaO ratio on crystallization, microstructure and dielectric properties of strontium titanate borosilicate glass ceramics. [doi: 10.1016/S0272-8842(03)00134-2]. Ceramics International, 30(3), 477-483.
15. Steckl, A. J., & Birkhahn, R. (1998). Visible emission from Er-doped GaN grown by solid source molecular beam epitaxy. Applied Physics Letters, 73(12), 1700-1702. doi: 10.1063/1.122250

16. Tanabe, S., Hayashi, H., Hanada, T., & Onodera, N. (2002). Fluorescence properties of Er3+ ions in glass ceramics containing LaF3 nanocrystals. [doi: 10.1016/S0925-3467(01)00236-1]. Optical Materials, 19(3), 343-349.
17. Thakur, O. P., Kumar, D., Parkash, O., & Pandey, L. (2002). Crystallization, microstructure development and dielectric behaviour of glass ceramics in the system [SrO · TiO2]-[2SiO2 · B2O3]-La2O3. Journal of Materials Science, 37(12), 2597-2606. doi: 10.1023/a:1015476631462
18. Thakur, O. P., Prakash, C., & James, A. R. (2009). Enhanced dielectric properties in modified barium titanate ceramics through improved processing. Journal of Alloys and Compounds, 470(1–2), 548-551. doi: http://dx.doi.org/10.1016/j.jallcom.2008.03.018
19. van den Hoven, G. N., Koper, R. J. I. M., Polman, A., van Dam, C., van Uffelen, J. W. M., & Smit, M. K. (1996). Net optical gain at 1.53 μm in Er-doped Al2O3 waveguides on silicon. Applied Physics Letters, 68(14), 1886-1888. doi: 10.1063/1.116283
20. Vetrone, F., Boyer, J.-C., Capobianco, J. A., Speghini, A., & Bettinelli, M. (2002). 980 nm excited upconversion in an Er-doped ZnO–TeO2 glass. Applied Physics Letters, 80(10), 1752-1754. doi: 10.1063/1.1458073
21. Xu, W., Dai, S., Toth, L. M., Del Cul, G. D., & Peterson, J. R. (1995). Green Upconversion Emission from Er3+ Ion Doped into Sol-Gel Silica Glasses under Red Light (647.1 nm) Excitation. [doi: 10.1021/j100013a013]. The Journal of Physical Chemistry, 99(13), 4447-4450. doi: 10.1021/j100013a013
22. Yi, G., Lu, H., Zhao, S., Ge, Y., Yang, W., Chen, D., & Guo, L.-H. (2004). Synthesis, Characterization, and Biological Application of Size-Controlled Nanocrystalline NaYF4: Yb, Er Infrared-to-Visible Up-Conversion Phosphors. [doi: 10.1021/nl048680h]. Nano Letters, 4(11), 2191-2196. doi: 10.1021/nl048680h
23. Zhang, J., Mi, C., Wu, H., Huang, H., Mao, C., & Xu, S. (2012). Synthesis of NaYF4: Yb/Er/Gd up-conversion luminescent nanoparticles and luminescence resonance energy transfer-based protein detection. [doi: 10.1016/j.ab.2011.11.008]. Analytical Biochemistry, 421(2), 673-679